Local structure of saccharose- and anthracene-based carbons studied by wide-angle high-energy X-ray scattering

ARTICLE *in* JOURNAL OF ALLOYS AND COMPOUNDS · JANUARY 2004

Impact Factor: 3 · DOI: 10.1016/S0925-8388(03)00604-2

Journal of Alloys and Compounds 362 (2004) 307–313

Journal of ALLOYS AND COMPOUNDS

www.elsevier.com/locate/jallcom

Local structure of saccharose- and anthracene-based carbons studied by wide-angle high-energy X-ray scattering

A. Szczygielska [a,*], A. Burian [a], J.C. Dore [b], V. Honkimäki [c], S. Duber [d]

[a] *Institute of Physics, University of Silesia Uniwersytecka 4, 40-007 Katowice, Poland*
[b] *School of Physical Sciences, University of Kent, Canterbury CT2 7NR, UK*
[c] *European Synchrotron Radiation Facility, BP 220, 38043 Grenoble Cedex 9, France*
[d] *Interdepartmental Laboratory of Structural Research, Faculty of Earth Sciences, University of Silesia, Ul. Będzińska 60, 41-200 Sosnowiec, Poland*

Received 17 June 2002; received in revised form 14 November 2002; accepted 20 January 2003

Abstract

A series of porous carbon materials, produced by pyrolysis of saccharose and anthracene and heat treated at 1000, 1900 and 2300 °C have been studied by wide-angle X-ray scattering. The X-ray data were collected at European Synchrotron Radiation Facility (ESRF) in Grenoble on the ID15A beam line (high-energy X-ray diffraction) using a wavelength of $E = 116.2$ keV, $\lambda = 0.1067$ Å. The data were recorded in the scattering vector range from 0.5 to 24 Å^{-1} which enabled them be converted to a real-space representation via the Fourier transform. The structure of these carbons has been described in terms of a model based on disordered, graphite-like layers with very weak interlayer correlations. At higher temperatures the anthracene-based carbon transforms into graphite while the carbon produced from saccharose remains disordered. The graphitization process has been studied in detail by careful analysis of the diffraction data in real and reciprocal space.

Keywords: Disordered systems; X-ray diffraction; Synchrotron radiation

1. Introduction

Elemental carbon exists in many forms of which diamond and graphite is the most familiar. The relatively recent discoveries of fullerenes and nanotubes have added to these well-known forms new materials consisting of large carbon molecules in which atoms are situated on curved surfaces. In addition to these ordered structures there is a wide range of disordered materials such as glassy or amorphous carbons, diamond-like carbons and activated porous carbons. The majority of these materials are usually prepared by carbonisation of organic precursors such as phenolic resin, polyfurfuryl alcohol, cellulose, anthracene, saccharose and natural products like olive or peach stones. Industrial productions of carbons began at the beginning of the twentieth century and since the 1930s the range of applications of porous carbons has expanded, encouraging ongoing research [1]. Today these carbons are used in a great number of applications in the chemical, pharmaceutical, food processing and other industries [2]. Porous carbons are also commonly used as catalysts and catalyst supports in oxidation, combination, decomposition and elimination reactions [3,4] and as electrodes in chemical sources of electricity [5].

It has been known for about a century that some carbon materials are more susceptible to graphitization than others. The first detailed study of graphitizing and non-graphitizing carbons, which can or cannot form graphite single-crystals after high-temperature heat treatment (3000 °C and above), was performed by Rosalind Franklin [1]. 'Non-graphitizing' carbons tend to be hard, low-density materials. They cannot be converted into graphite and are characterised by strong cross-linking between the basic building blocks and form a rigid, isotropic and highly porous structure. 'Graphitizing carbons' are soft, less porous, with densities much closer to that of crystalline graphite. They are characterised by anisotropic properties due to their structure consisting of a layer sequence [6].

* Corresponding author. Tel./fax: +48-32-258-8431.
E-mail address: aszczyg@us.edu.pl (A. Szczygielska).

0925-8388/$ – see front matter © 2003 Elsevier B.V. All rights reserved.
doi:10.1016/S0925-8388(03)00604-2

Although these materials have been studied by X-ray, electron and neutron diffraction, which are the most direct probes of their structures, the interpretation of experimental data and the explanation of the different behaviour of these materials upon annealing is rather complicated due to the interplay of order and disorder in interatomic correlations. Therefore the formalism of classical crystallography fails in this case and new interpretation methods are needed. In order to understand the structure of such kind of materials it is necessary to determine the atomic arrangement within a single layer and also the inter-layer correlations.

The purpose of the present work is to trace changes in the structure of two disordered carbons obtained from anthracene (graphitizing) and saccharose (non-graphitizing) versus temperature of heat treatment.

2. Experimental

2.1. Sample preparation

The carbons studied in the present work were prepared by the pyrolysis of anthracene ($C_{14}H_{10}$) and saccharose ($C_{12}H_{22}O_{11}$). Sample preparation consisted of three steps. First, the coke from anthracene and saccharose at temperatures 230 and 400 °C was prepared and then the obtained black substances were crumbed to about 1 mm grain size. In the next stage, the samples were heated from room temperature to 1000 °C and annealed in the final temperature for half an hour. In the last stage, both samples made from anthracene and from saccharose were heated up to 1900 and 2300 °C and then also annealed at these temperatures for half an hour. This treatment was carried out under argon atmosphere. The carbonization process, performed at the above indicated temperature, removed almost all non-carbon components from the samples [7].

2.2. X-ray scattering measurement

The high-energy X-ray scattering experiment were performed on the ID15A beam-line at the European Synchrotron Radiation Facility (ESRF, Grenoble). The photon energy $E = 116.2$ keV ($\lambda = 0.1067$ Å) was used for the measurements. The powdered samples were placed in capillary tubes of 3 mm diameter and mounted on the diffractometer axis. The intensities were recorded using a Ge solid-state detector. The measured intensities cover a K-range up to 24 $Å^{-1}$ [7]. The intensity scattered by the empty capillary was measured separately and was subtracted from the experimental data.

Two-dimensional diffraction patterns were also recorded on the ID15B beam line at ESRF using the imaging plate as the detector. Weak effect of texture was observed only for the anthracene-based carbons annealed at higher temperatures. Such a test has shown that the present results are not obscured by the preferred orientation effects [8]. The experimental data were normalized to electron units using the high-angle method followed by subtraction of the Compton intensity. The intensities were also recorded for natural graphite for comparison.

3. Theoretical background

The anthracene- and saccharose-based carbons studied in this work are disordered and their structure is through an assembly of ordered regions, randomly distributed in space. In the case of scattering by a disordered system, the intensity distribution, averaged over all orientations, can be described by Debye's equation as follows:

$$I_0(K) = \left\langle \frac{1}{N} \sum_{k=1}^{N} \sum_{l=1}^{N} f_k f_l \mathrm{e}^{-i(\boldsymbol{K}\boldsymbol{r}_{ij})} \right\rangle_{\text{allorientations}} = \frac{1}{N} \sum_{k=1}^{N} \sum_{l=1}^{N} f_k f_l \left(\frac{\sin(Kr_{kl})}{Kr_{kl}} \right) \quad (1)$$

where: $K = 4\pi(\sin\theta)/\lambda$ is the scattering vector, 2θ is the scattering angle, λ is the wavelength, N indicates the number of atoms, f_k, is the atomic scattering factor of the K-atom, and r_{kl} denotes the distance between the kth and lth atoms. For the modelling of the structure of the porous carbons the Debye equation, normalized to one atom, was used. Attenuation of the intensity due to structural disorder (thermal vibration of atoms and static disorder) is taken into account by including the Debye–Waller type term and finally the intensity per atom is given by:

$$I(K) = \frac{1}{N} f^2 \sum_{k=1}^{N} \sum_{l=1}^{N} \left(\frac{\sin(Kr_{kl})}{Kr_{kl}} \right) \exp\left(-\frac{\sigma_{kl}^2 K^2}{2} \right) \quad (2)$$

The spatial correlations between atoms or particles leading to interference of the scattered waves give rise to the structure factor $S(K)$, which modulates the scattered intensity, providing information about the structure of investigated materials through analysis in reciprocal space. The structure factor (SF) is defined as follows:

$$S(K) = \frac{I(K)}{f^2}. \quad (3)$$

From Eqs. (2) and (3) one can readily obtain:

$$S(K) = \left[\frac{1}{N} \sum_{k=1}^{N} \sum_{l=1}^{N} \frac{\sin(Kr_{kl})}{(Kr_{kl})} \right]_{k \neq l} \exp\left(-\frac{\sigma_{kl}^2 K^2}{2} \right) + 1 \quad (4)$$

The structure factor $S(K)$ is independent of the scattering power of individual atoms and depends only on the structure of the investigated sample. The scattering data can be converted to real space by the inverse Fourier transform of $S(K)$ yielding the reduced radial distribution function $d(r)$

(RRDF), which is defined as:

$$d(r) = 4\pi\rho_0[g(r) - 1] = \frac{2}{\pi} \times \int_0^{K_{\max}} K[S(K) - 1]W(K)\sin(Kr)\mathrm{d}K \quad (5)$$

where ρ_0 is the number density and $W(K)$ is the Lorch window function [9]:

$$W(K) = \frac{\sin\left(\frac{\pi K}{K_{\max}}\right)}{\left(\frac{\pi K}{K_{\max}}\right)}, \quad (6)$$

which is included to allow for truncation effects of the experimental data at $K_{\max}$, $g(r)$ is called the pair correlation function. The experimental RRDF provides information about the probability of finding an atom in a spherical shell at a distance r from an arbitrary atom. Successive peaks correspond to nearest-, second- and next-neighbour atomic distribution.

The structure of the investigated carbons will be described in the present work in terms of the paracrystalline model within a single graphitic layer and in the c-axis direction. The paracrystalline model is based on the assumption that the distances from any atoms to adjacent atoms fluctuate without statistical correlations and that these fluctuations propagate proportionally to square root of the interatomic distance according to the combination law of independent probability distributions of the Gaussian type. The paracrystalline theory [10,11] implies the so-called '$\alpha*$ *-relation*' which is expressed as:

$$\alpha* = \sqrt{N_l}g, \quad (7)$$

where $0.10 \leq \alpha^* \leq 0.20$ and N_l indicates the average number of netplanes in the paracrystal.

$$g = \frac{\Delta d_c}{d_c} = \sqrt{\frac{\langle d_c^2\rangle - \langle d_c\rangle^2}{\langle d_c\rangle^2}} \quad (8)$$

is the relative statistical deviation of the interplanar spacing d_c in the paracrystal, d_c is the interplanar distance for the net-planes with the highest density of atoms and $\langle\,\rangle$ indicates the statistical average value of the quantity in the brackets. The relation (7) has the physical meaning, that real paracrystals have a limited size, controlled by the degree of disorder specified by g and that the surface net-planes have a statistical roughness of 0.10–0.20 of the net-plane distance. In other words, large paracrystals are not strongly disordered.

4. Modelling procedure

The model of the structure is defined by the Cartesian coordinates of the atoms from which the model is built up. Such an approach allows to compute the scattering factor related directly to the intensity by Eq. (3) and to compare the results of the simulations with the experimental data in reciprocal space. The model parameters are: the lattice constants a and c of the graphitic structure, the radius of the limiting circle R_a, defining the model size within a single graphitic layer, the generalized Debye–Waller factor with $\sigma_{\text{intra}} = \sigma_1 + \sigma_0\sqrt{r}$ for the atoms laying on an isolated layer and the number of layers in sequence N_l. The linear increase of σ_{intra} with $\sqrt{r}$ can be explained in terms of the paracrystalline structure within a single layer, according to Refs. [10,11]. The lattice constant: $a = 2.456$ Å and $c = 7.20$, 6.88, 6.84 Å for the saccharose-based carbons and $c = 6.90$, 6.74, 6.74 Å for the anthracene-based carbons were taken for computation both at 1000, 1900 and 2300 °C, respectively. At this stage of modelling the set of the Cartesian coordinates has been generated on the base of the input model parameters for the graphite structure. Then the graphite structure was disordered by successive shifts of graphitic layers from their original positions by the translation vectors $(\Delta\vec{x}, \Delta\vec{y})$ defined as random numbers from $(-\frac{a}{2}, \frac{a}{2})$ range. Paracrystalline stacking of layers was simulated assuming the Gaus-

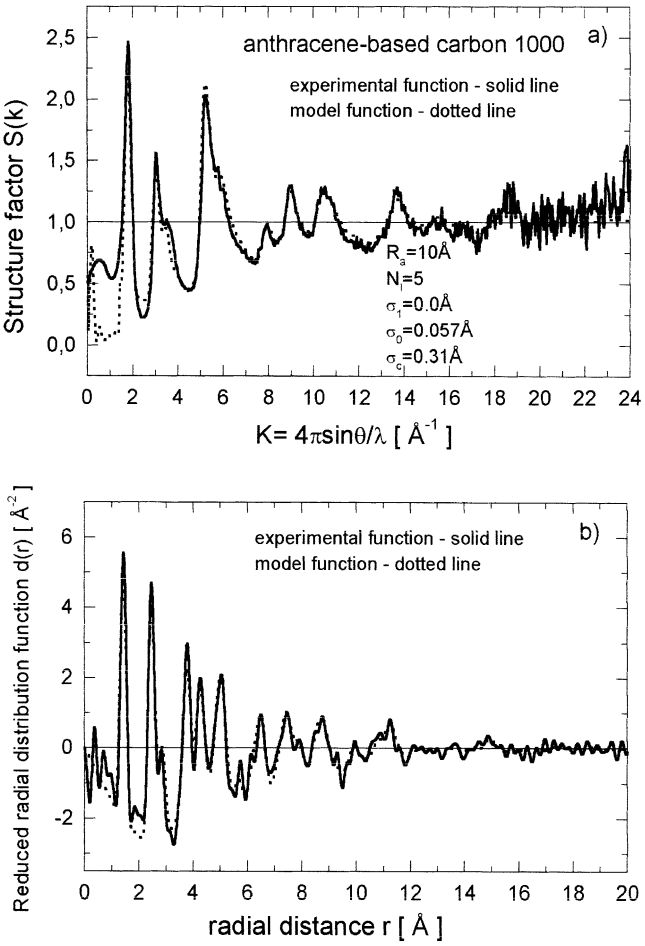

Fig. 1. (a) The experimental (solid line) and simulated as described in Section 4 (dotted line) structure factors $S(K)$ of the anthracene-based carbon annealed at 1000 °C. (b) Their Fourier transforms computed according to Eq. (5) (the experimental (solid line) and simulated (dotted line) $d(r)$ functions).

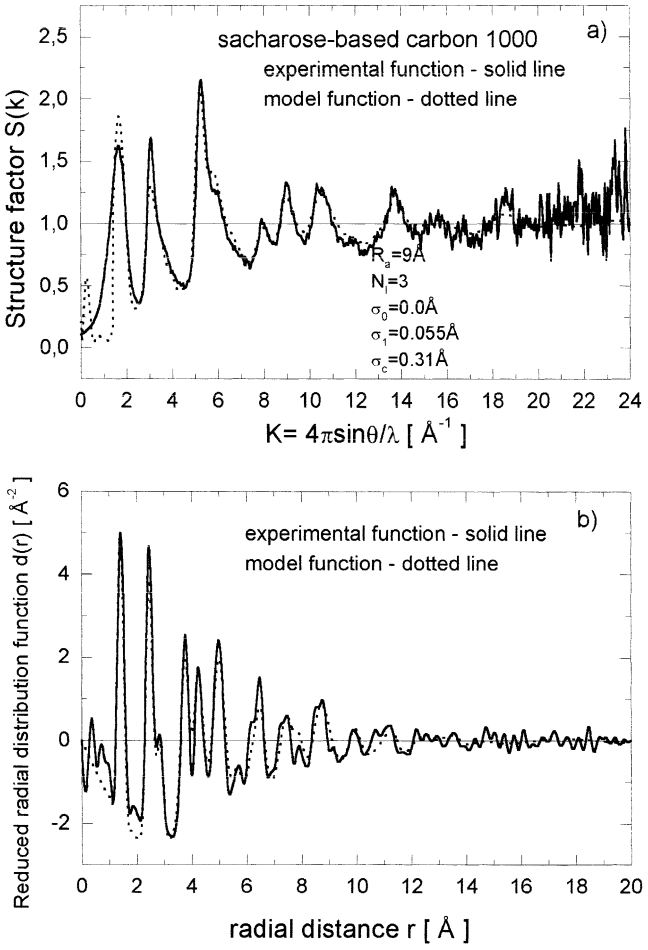

Fig. 2. (a) The experimental (solid line) and simulated as described in Section 4 (dotted line) structure factors $S(K)$ of the saccharose-based carbon annealed at 1000 °C. (b) Their Fourier transforms computed according to Eq. (5) (the experimental (solid line) and simulated (dotted line) $d(r)$ functions).

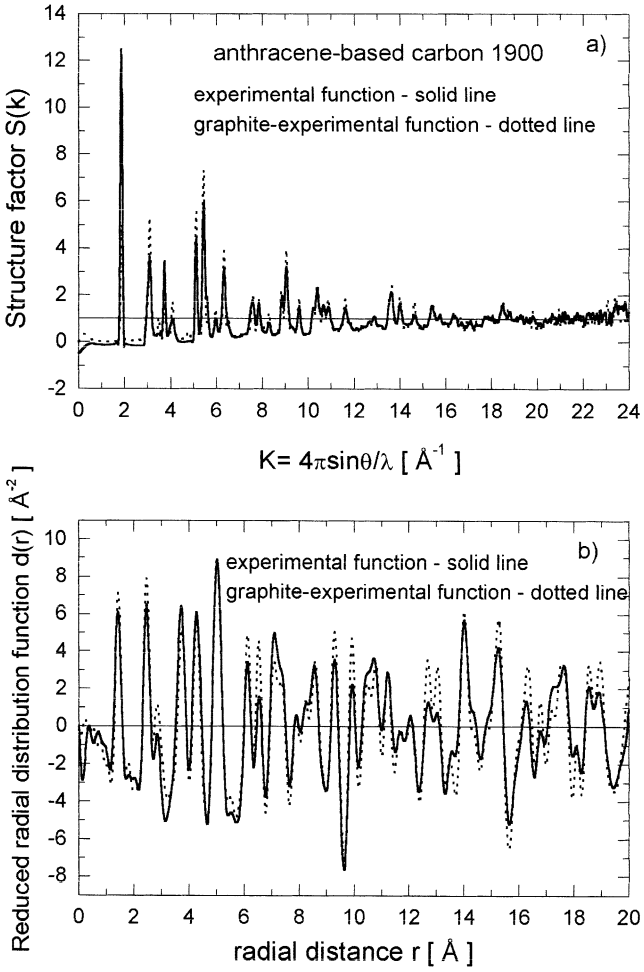

Fig. 3. (a) The experimental (solid line) and simulated as described in Section 4 (dotted line) structure factors $S(K)$ of the anthracene-based carbon annealed at 1900 °C. (b) Their Fourier transforms computed according to Eq. (5) (the experimental (solid line) and simulated (dotted line) $d(r)$ functions).

sian distribution of the interlayer spacing. The random numbers with the Gaussian distribution were generated as the sum of the random numbers with uniform distribution over the (0,1) range, appropriately normalized according to the central limit theorem. The standard deviation of the interlayer spacing is denoted by σ_c. The structure factors were computed for 200 simulated atomic arrangements and then averaged. Finally, the simulated structure factors were converted to real space via the Fourier transform. The numerical procedure is described in detail in Ref. [12] where the structure of the activated carbons prepared from phenolic resin has been investigated.

5. Results and discussion

The results of paracrystalline simulations for the anthracene- and saccharose-based carbons, annealed at 1000 °C are compared with the experimental data in Fig. 1 in both reciprocal (a) and real (b) space. The model parameters are listed in Table 1. The SFs and the RRDFs of both carbons at 1000 °C are very similar and typical for heavily disordered materials called turbostratic carbons [13]. The main difference between the anthracene and saccharose-based carbons is in the amplitude of the first (002) type diffraction peak, clearly higher for the former. The amplitude of this peak is related to the number of the netplanes in stacking and its position Q_1 gives the inter-planar spacing $d_c = c/2 = 2\pi/Q_1$. The values of d_c for the saccharose-based carbon (3.60 Å) is clearly greater than that of graphite (3.35 Å). A much smaller difference is observed in the case of the anthracene-based carbon (3.45 Å). From the comparison of the experimental and simulated curves in Figs. 1 and 2, it can be concluded that the turbostratic model with the paracrystalline distortion within a single layer and in layer stacking reproduces very well all the peak positions, amplitudes and shapes of the experimental functions, both in real and reciprocal space. The model size in the direction perpendicular to the

Table 1
The structural parameters obtained for anthracene- and saccharose-based carbons

	Anthracene-based carbon				Saccharose-based carbon			
	R_a (Å)	N_l	σ_{intra}	σ_c	R_a (Å)	N_l	σ_{intra}	σ_c
1000 °C	10	5	$\sigma_1 = 0.00$ $\sigma_0 = 0.057$	0.31	9	3	σ_1=0.00 $\sigma_0 = 0.055$	0.31
1900 °C	–	–	–	–	20	6	σ_1=0.03 σ_0=0.004	0.09
2300 °C	–	–	–	–	25	9	σ_1=0.038 σ_0=0.002	0.07

layers is for the anthracene-based carbon about twice of that of the saccharose-based carbon. The size of the ordered regions within a single layer were assumed to be about 10 Å, both of the anthracene- and saccharose-based carbon heated at 1000 °C. At higher temperatures both investigated carbons exhibit completely different behaviour. At 1900 °C the structure factor and the reduced radial distribution function of the anthracene-based carbon, shown in Fig. 3, are very close to those of graphite. However, small differences in the peak amplitudes can be seen in Fig. 3a,b. It suggests that the graphitization process starts at this temperature. The structure of the anthracene-based carbon annealed at 1900 °C cannot be described by the turbostratic model with the paracrystalline distortion. On the contrary, the carbon produced from the saccharose at this temperature remains disordered. The model size increase within a single layer and in the direction perpendicular to layers. A degree of the

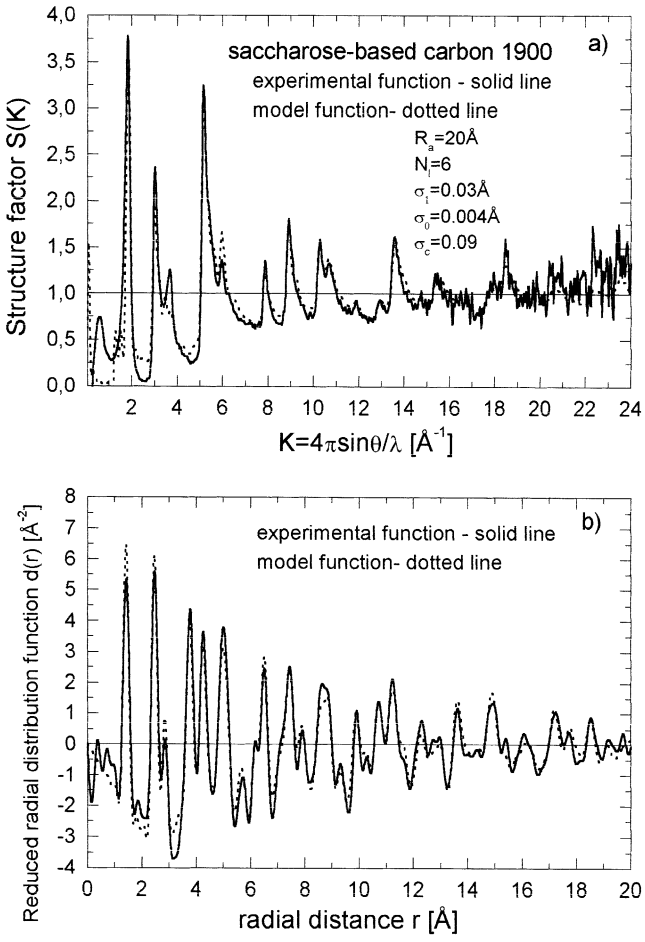

Fig. 4. (a) The experimental (solid line) and simulated as described in Section 4 (dotted line) structure factors $S(K)$ of the saccharose-based carbon annealed at 1900 °C. (b) Their Fourier transforms computed according to Eq. (5) (the experimental (solid line) and simulated (dotted line) $d(r)$ functions).

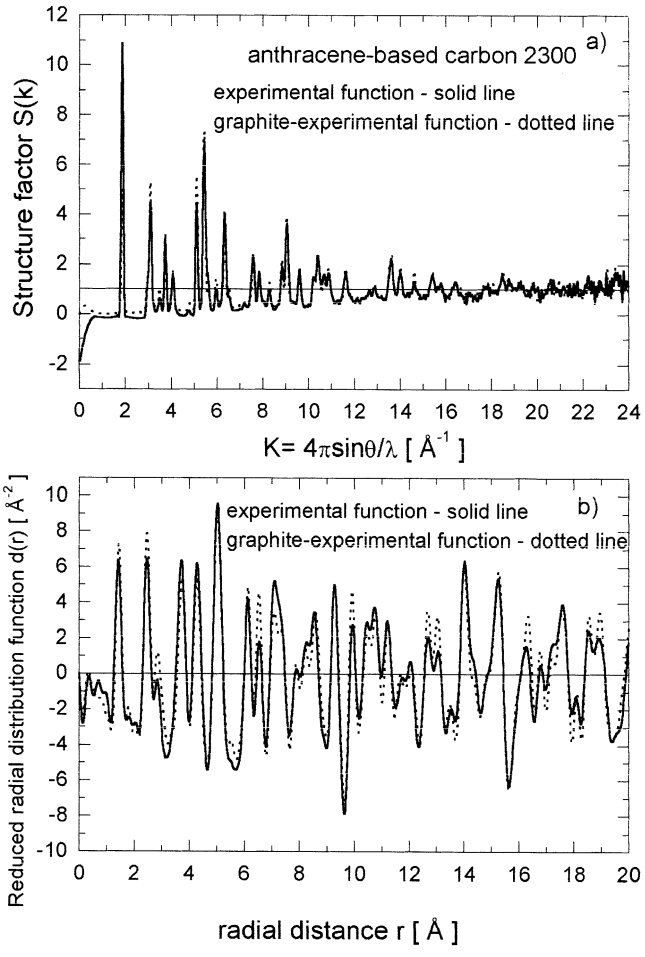

Fig. 5. (a) The experimental (solid line) and simulated as described in Section 4 (dotted line) structure factors $S(K)$ of the anthracene-based carbon annealed at 2300 °C. (b) Their Fourier transforms computed according to Eq. (5) (the experimental (solid line) and simulated (dotted line) $d(r)$ functions).

network distortion, described by σ_1, σ_0, and σ_c, is significantly lower as can be seen from Table 1. The model-based simulation with the structure parameters listed in Table 1 reproduces reasonably well the positions and shapes of peaks of the experimental functions in Fig. 4. At 2300 °C the anthracene-based carbon transforms almost completely into graphite as it can be seen in Fig. 5, where an overall agreement of the $S(K)$ and $d(r)$ functions of the carbon produced from anthracene and of graphite is good. Remaining discrepancies can be explained by defects in the structure of the annealed sample. Heating at this relatively high temperature does not lead to graphitization of the carbon produced from saccharose, which can be seen in Fig. 6. The turbostratic model with the paracrystalline distortion results in a good fit to the experimental data. The model sizes are slightly increased and the paracrystalline distortions are relaxed in comparison with the sample heated at 1900 °C. These results indicate resistance of the saccharose-based carbons to graphitization and support the previous findings reached by careful high resolution electron microscopy observations [14,15] and our pulsed neutron diffraction studies [8].

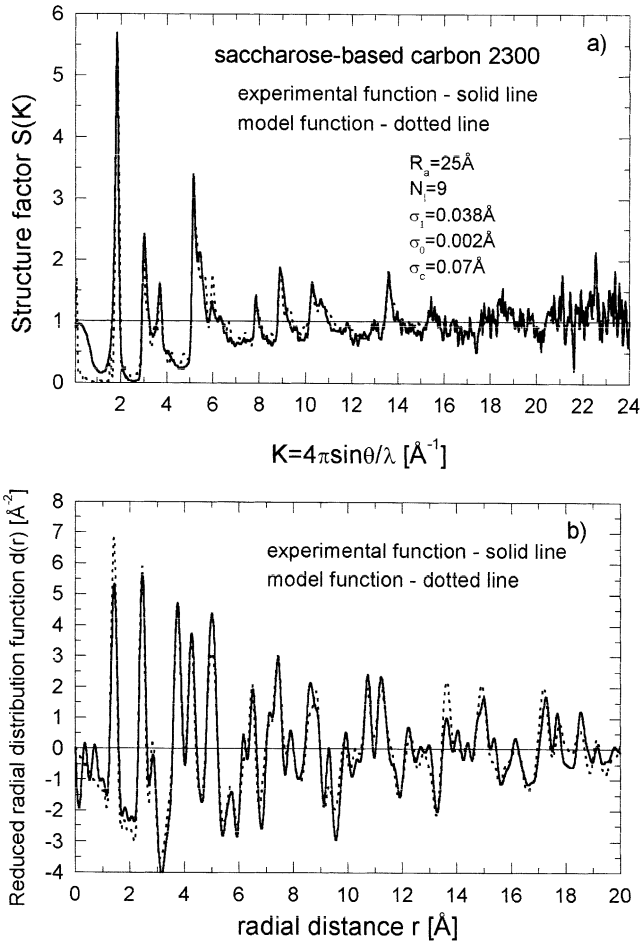

Fig. 6. (a) The experimental (solid line) and simulated as described in Section 4 (dotted line) structure factors $S(K)$ of the saccharose-based carbon annealed at 2300 °C. (b) Their Fourier transforms computed according to Eq. (5) (the experimental (solid line) and simulated (dotted line) $d(r)$ functions).

6. Conclusions

The high energy X-ray scattering experiment, performed using synchrotron radiation, yielded the experimental data of good quality, which can be numerically analysed. This analysis demonstrates that the structure of the saccharose-based carbons at 1000, 1900 and 2300 °C and the anthracene-based carbon at 1000 °C cannot be described in terms of the structure of the three-dimensional graphite. The turbostratic model with the paracrystalline distortion within a single layer and in layer stacking describes the structure of these samples, which consists of the small ordered regions randomly oriented in space. The carbons produced from saccharose are clearly non-graphitizing, whereas the anthracene-based carbon can be easily converted into graphite under the high temperature heat treatment and their structure can be described on the basis of a graphitic structure. It can be also concluded that, together with the temperature, the size of the correlations increase both within a single layer and in the *c*-axis direction. So the ordered domains grow up together with the temperature. These results confirm Oberlin's suggestions based on the electron microscopy investigations [16]. The results of the present work are also in agreement with our earlier electron microscopy and Raman scattering studies in which the presence of fullerene- and nanotube-like fragments in such produced carbons has been suggested [16–18].

Acknowledgements

The work was supported by the State Committee for Scientific Research (KBN) grant no 5 PO3B 113 21.

References

[1] I. Mochida, S. Kawano, S. Kisamori, Fujitsu, T. Maeda, Carbon 32 (1994) 175.
[2] R.C. Bansal, J.-B. Donnet, F. Stoeckli, in: Active Carbon, Marcel Dekker, New York, 1988.
[3] J. Klinik, T. Grzybek, Fuel 71 (1992) 303.
[4] M. Molina-Sabi, V. Perez, F. Rodriguez-Reinoso, Carbon 32 (1994) 1259.
[5] H. Jankowska, A. Swiątkowski, J. Choma, in: Active Carbon, Ellis Horwood, Chichester, UK, 1991.
[6] R.E. Franklin, Proc. R. Soc. A 209 (1951) 196.
[7] A. Szczygielska, A. Burian, S. Duber, J.C. Dore, V. Honkimaki, J. Alloys Comp. 328 (2001) 231–236.
[8] A. Szczygielska, PhD Thesis: Characterization of spatial correlations between atoms for non-crystalline carbons, University of Silesia, Poland, 2002.
[9] E.A. Lorch, J. Phys. C 2 (1969) 229.
[10] R. Hosemann, S.N. Bagchi, in: Direct Analysis of Diffraction by Matter, North Holland, Amsterdam, 1962, p. 69.

[11] A.M. Hindeleh, R. Hosemann, J. Phys. C (Solid State Phys.) 21 (1988) 4155.
[12] A. Szczygielska, A. Burian, J.C. Dore, J. Phys.: Condens. Matter 13 (2001) 5545–5561.
[13] B.E. Warren, Phys. Rev. 9 (1941) 693.
[14] A. Oberlin, Carbon 22 (1984) 521.
[15] J. Goma, A. Oberlin, Thin Solid Films 65 (1980) 221–232.
[16] P.J.F. Harris, A. Burian, S. Duber, Phil. Mag. Lett. 80 (6) (2000) 381–386.
[17] A. Burian, J.C. Dore, Acta Phys. Polon. A 98 (2000) 457.
[18] A. Burian, Ph. Daniel, S. Duber, J.C. Dore, Phil. Mag. B 81 (2001) 525.